Article

Self-Assembly of Discotic Mesogens in Solution and in Liquid Crystalline Phases: Effects of Substituent Position and Hydrogen Bonding

Christine Lavigueur, E. Johan Foster, and Vance E. Williams

J. Am. Chem. Soc., **2008**, 130 (35), 11791-11800 • DOI: 10.1021/ja803406k • Publication Date (Web): 12 August 2008

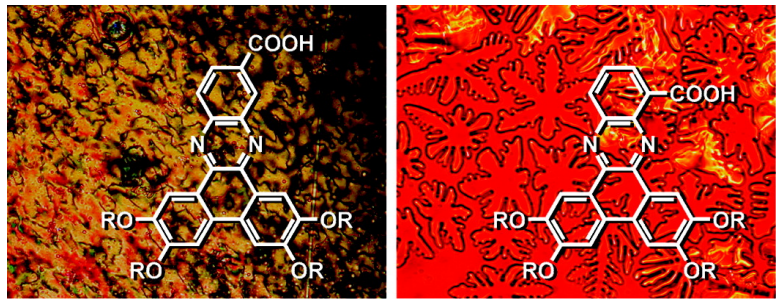

More About This Article

Additional resources and features associated with this article are available within the HTML version:

- Supporting Information
- Access to high resolution figures
- Links to articles and content related to this article
- Copyright permission to reproduce figures and/or text from this article

View the Full Text HTML

J|A|C|S
ARTICLES

Published on Web 08/12/2008

Self-Assembly of Discotic Mesogens in Solution and in Liquid Crystalline Phases: Effects of Substituent Position and Hydrogen Bonding

Christine Lavigueur, E. Johan Foster, and Vance E. Williams*

4D LABS and Department of Chemistry, Simon Fraser University, 8888 University Drive, Burnaby, British Columbia, Canada, V5A 1S6

Received May 7, 2008; E-mail: vancew@sfu.ca

Abstract: The effects of functional group position on the phase behavior of discotic mesogens was examined for a series of dibenzophenazine derivatives bearing a carboxylic acid, methyl carboxylate, or nitro group. In all cases, changing the position of the group from the "top" to the "side" of the aromatic core led to dramatic differences in the phase behavior, both in terms of the stability of the liquid crystalline phases as well as the types of mesophases formed. For the non-hydrogen bonding ester and nitro derivatives, moving the substituent to the side of the core led to a lowering of the clearing temperatures or loss of liquid crystallinity. Carboxylic acid derivatives exhibit broad mesophases irrespective of the position of the acid group, but mesogens bearing this group on the side of the core exclusively form Col_h phases, whereas those with an acid group on the top of the core exhibit more varied mesomorphism, with the formation of Col_h, Col_r, and nematic phases. Contrary to expectations, the presence of a carboxylic acid group on the side of the core does not appear to lead to the formation of dimeric structures in the liquid crystalline phase, although the columnar structures appear to be stabilized by intermolecular hydrogen bonding along the columns. These derivatives also form π-stacked dimers in solution; the structure of these dimers are consistent with the proposed structure of the columnar phases.

Introduction

Until recently, few molecular shapes were considered compatible with the formation of liquid crystalline phases, with rod-shaped (calamitic) and disc-shaped (discotic) mesogens receiving by far the most attention. This preconception has largely been dispelled by the rapid development of unconventionally shaped mesogens such as bent-rod,[1] polycatenar,[2] tetrahedral,[3] octahedral,[3] bowlic,[4] dendritic,[5] T-shaped,[6] and ring-shaped[7] molecules. This newly discovered structural diversity highlights how much of mesogenic "shape space" has yet to be explored. For example, elliptical mesogens, which can be regarded as intermediate forms between calamitic and discotic mesogens, have received surprisingly little attention. While there are several structural motifs that can be regarded as roughly elliptical,[8−10] one particularly convenient way to assemble mesogens with this shape is by rigidly linking together two disc-shaped components.[11−13] In this context, we recently examined a series of disc-shaped compounds (series **tA**) that hydrogen bond to form elliptical dimers, which in turn organize into a variety of columnar and nematic mesophases.[11] The presence of a car-

(1) (a) Reddy, R. A.; Tschierske, C. *J. Mater. Chem.* **2006**, *16*, 907–961. (b) Ros, M. B.; Serrano, J. L.; de la Fuente, M. R.; Folcia, C. L. *J. Mater. Chem.* **2005**, *15*, 5093–5098. (c) Takezoe, H.; Takanishi, Y. *Jpn. J. Appl. Phys., Part 1* **2006**, *45*, 597–625.

(2) (a) Gharbia, M.; Gharbi, A.; Nguyen, H. T.; Malthête, J. *Curr. Opin. Colloid Interface Sci.* **2002**, *7*, 312–325. (b) Nguyen, H. T.; Destrade, C.; Malthête, J. In *Handbook of Liquid Crystals*; Demus, D., Goodby, J., Gray, G. W., Spiess, H.-W., Vill, V., Eds.; Wiley-VCH: Weinheim, Germany, 1998; Vol. 2B, p 865−885.

(3) Tschierske, C. *J. Mater. Chem.* **1998**, *8*, 1485–1508.

(4) (a) Tschierske, C. *Annu. Rep. Prog. Chem., Sect. C* **2001**, *97*, 191–267. (b) Abis, L.; Arrighi, V.; Cometti, G.; Dalcanale, E.; Du Vosel, A. *Liq. Cryst.* **1991**, *9*, 277–284. (c) Cometti, G.; Dalcanale, E.; Du Vosel, A.; Levelut, A. M. *J. Chem. Soc., Chem. Commun.* **1990**, 163–165.

(5) (a) Donnio, B.; Buathong, S.; Bury, I.; Guillon, D. *Chem. Soc. Rev.* **2007**, *36*, 1495–1513. (b) Marcos, M.; Martín-Rapún, R.; Omenat, A.; Serrano, J. L. *Chem. Soc. Rev.* **2007**, *36*, 1889–1901. (c) Ponomarenko, S. A.; Rebrov, E. A.; Bobrovsky, A. Yu.; Boiko, N. I.; Muzafarov, A. M.; Shibaev, V. P. *Liq. Cryst.* **2006**, *33*, 1497–1512.

(6) (a) Bae, W.-S.; Lee, J.-W.; Jin, J.-I. *Liq. Cryst.* **2001**, *28*, 59–67. (b) Zuev, V. V. *Russ. J. Gen. Chem.* **2007**, *77*, 1266–1270.

(7) (a) Mindyuk, O. Y.; Stetzer, M. R.; Heiney, P. A.; Nelson, J. C.; Moore, J. S. *Adv. Mater.* **1998**, *10*, 1363–1366. (b) Höger, S.; Enkelmann, V.; Bonrad, K.; Tschierske, C. *Angew. Chem., Int. Ed. Engl.* **2000**, *39*, 2268–2270.

(8) (a) Fernández, O.; de la Torre, G.; Fernández-Lázaro, F.; Barberá, J.; Torres, T. *Chem. Mater.* **1997**, *9*, 3017–3022. (b) Seo, J.; Kim, S.; Gihm, S. H.; Park, C. R.; Park, S. Y. *J. Mater. Chem.* **2007**, *17*, 5052–5057.

(9) For examples of mesogens that could be regarded as approximately elliptical but were not described that way in the original report, see: (a) Bilgin-Eran, B.; Tschierske, C.; Diele, S.; Baumeister, U. *J. Mater. Chem.* **2006**, *16*, 1145–1153. (b) Ohta, K.; Higashi, R.; Ikejima, M.; Yamamoto, I.; Kobayashi, N. *J. Mater. Chem.* **1998**, *8*, 1979–1991. (c) Chen, Z.; Baumeister, U.; Tschierske, C.; Würthner, F. *Chem.—Eur. J.* **2007**, *13*, 450–465. (d) Nolde, F.; Pisula, W.; Müller, S.; Kohl, C.; Müllen, K. *Chem. Mater.* **2006**, *18*, 3715–3725. (e) Würthner, F. *Chem. Commun.* **2004**, 1564–1579.

(10) Some mesogens described as rectangular, boardlike, or sanidic could also be considered to have a roughly elliptical shape, see: (a) Szydłowska, J.; Krówczyński, A.; Bilewicz, R.; Pociecha, D.; Głaz, Ł. *J. Mater. Chem.* **2008**, *18*, 1108–1115. (b) Artal, M. C.; Toyne, K. J.; Goodby, J. W.; Barberá, J.; Photinos, D. J. *J. Mater. Chem.* **2001**, *11*, 2801–2807. (c) Haristoy, D.; Méry, S.; Heinrich, B.; Mager, L.; Nicoud, J.-F.; Guillon, D. *Liq. Cryst.* **2000**, *27*, 321–328. (d) Méry, S.; Haristoy, D.; Nicoud, J.-F.; Guillon, D.; Diele, S.; Monobe, H.; Shimizu, Y. *J. Mater. Chem.* **2002**, *12*, 37–41.

Scheme 1. General Synthesis of Compounds **tA**, **sA**, **tE**, **sE**, **tN**, and **sN**

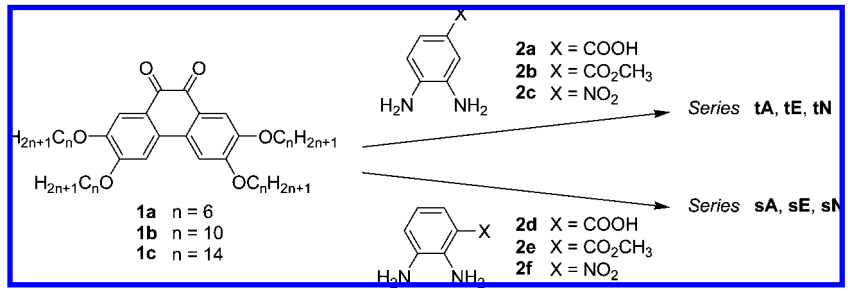

boxylic acid group plays an essential role in the liquid crystalline properties of these compounds, as was demonstrated by the markedly different phase behavior of related molecules that lack the ability to form hydrogen bonds.

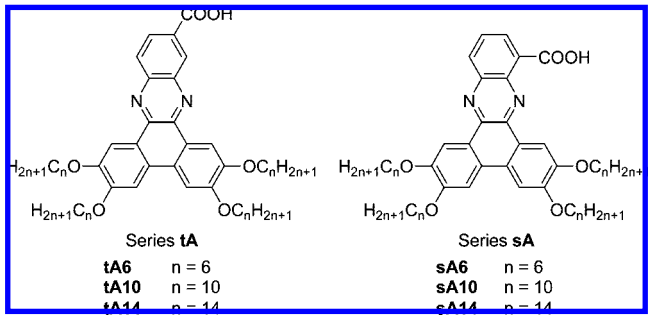

The location of these acid groups presumably has a significant impact on mesophase behavior, since changing their position would dramatically alter the geometry of any resulting dimers. In the present study, we examine the effects of moving the carboxylic acid group from the "top" (**t**) of the molecule in series **tA** to the "side" (**s**) in series **sA**. To better understand the effects of hydrogen bonding on the properties of these compounds, a series of methyl ester analogues (series **tE** and **sE**) of similar size, shape, and electronic properties, but without the capability to form hydrogen-bonded dimers, were also prepared.

More broadly, while the nature of a functional group attached to the aromatic core of a discotic mesogen has been shown to strongly influence liquid crystalline properties,[14−18] the effects of substituent position has not been systematically investigated. Because clearing temperature has been shown to be correlated to the electron-withdrawing ability of a substituent attached to the core, derivatives with a nitro group are expected to exhibit among the highest clearing temperatures within a series of mesogens that lack the ability to form hydrogen bonds. Compounds in series **tN** and **sN** were therefore prepared as benchmarks for comparison with both the ester and acid derivatives described above. It was also anticipated that the nitro and ester derivatives would provide insight into the effects of changing the position of non-hydrogen bonding functional groups on mesophase behavior.

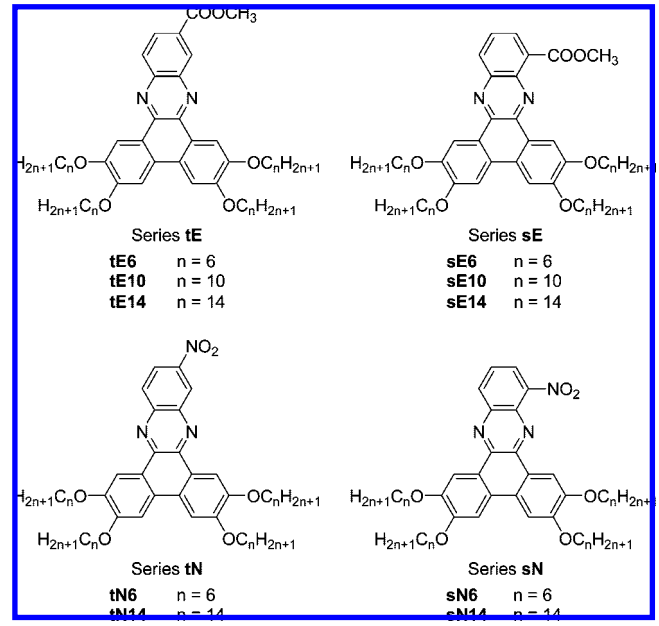

Early in the course of these studies, it was noted that the ^{1}H NMR spectra of all molecules in series **sA** showed a marked concentration dependence, which is a sign of self-assembly in solution. The solution behavior of the molecules in series **sA** and **sE** was therefore investigated.

Results and Discussion

Synthesis. The synthesis and phase behavior of compounds **tN6**, **tE6**, **tE10**, **tA6**, and **tA10** have been previously reported.[11,16] Compounds **tN14**, **sN6**, **sN14**, **tE14**, **sE6**, **sE10**, **sE14**, **sA6**, and **sA10** were each prepared by condensation of the appropriate diamine with a 2,3,6,7-tetrakis(alkoxy)-phenanthrene-9,10-dione, as shown in Scheme 1. This previously developed modular approach allows the rapid assembly of disc-shaped molecules having the desired chain length and functional group.[11,13,16−20] The diamines **2a**, **2c**, and **2f** were obtained commercially, while

(11) Foster, E. J.; Lavigueur, C.; Ke, Y. C.; Williams, V. E. *J. Mater. Chem.* **2005**, *15*, 4062–4068.
(12) (a) Kumar, S.; Varshney, S. K. *Liq. Cryst.* **2001**, *28*, 161–163. (b) Kumar, S.; Varshney, S. K. *Org. Lett.* **2002**, *4*, 157–159.
(13) Lavigueur, C.; Foster, E. J.; Williams, V. E. *Liq. Cryst.* **2007**, *34*, 833–840.
(14) Cammidge, A. N.; Bushby, R. J. In *Handbook of Liquid Crystals*; Demus, D., Goodby, J., Gray, G. W., Spiess, H.-W., Vill, V., Eds.; Wiley-VCH: Weinheim, Germany, 1998; Vol. 2B, p 693−748.
(15) (a) Kumar, S. *Liq. Cryst.* **2004**, *31*, 1037–1059. (b) Debije, M. G.; Chen, Z.; Piris, J.; Neder, R. B.; Watson, M. M.; Müllen, K.; Würthner, F. *J. Mater. Chem.* **2005**, *15*, 1270–1276. (c) Feng, X.; Pisula, W.; Zhi, L.; Takase, M.; Müllen, K. *Angew. Chem., Int. Ed. Engl.* **2008**, *47*, 1703–1706.
(16) Foster, E. J.; Jones, R. B.; Lavigueur, C.; Williams, V. E. *J. Am. Chem. Soc.* **2006**, *128*, 8569–8574.
(17) Babuin, J.; Foster, J.; Williams, V. E. *Tetrahedron Lett.* **2003**, *44*, 7003–7005.
(18) Mohr, B.; Wegner, G.; Ohta, K. *J. Chem. Soc., Chem. Commun.* **1995**, 995–996.
(19) (a) Foster, E. J.; Babuin, J.; Nguyen, N.; Williams, V. E. *Chem. Commun.* **2004**, 2052–2053. (b) Ong, C. W.; Hwang, J.-Y.; Tzeng, M.-C.; Liao, S.-C.; Hsu, H.-F.; Chang, T. H. *J. Mater. Chem.* **2007**, *17*, 1785–1790.
(20) Wenz, G. *Makromol. Chem., Rapid Commun.* **1985**, *6*, 577–584.

2b, **2d**, and **2e** were prepared using modified literature procedures.[16,21] Quinones **1a** and **1b** were synthesized as previously reported,[17,20,22] and **1c** was prepared following the same general procedure.

Attempts to synthesize **tA14** and **sA14** by the direct condensation of **1c** with the benzoic acid derivatives **2a** and **2d** proved to be inefficient. Although crude **tA14** was obtained in good yields by this method, its extremely low solubility made it very difficult to purify. Condensation of quinone **1c** with 2,3-diaminobenzoic acid **2d** led to an approximately 1:2 mixture of **1c** and the desired product, **sA14**. This mixture was almost impossible to separate even after repeated column chromatography and recrystallizations, possibly due to the formation of a complex between the two species. Indeed, a mixture of **sA14** and the quinone **1c** almost invariably resulted in a single spot by TLC, with an R_f that did not correspond to that of pure **1c**. To circumvent these problems, **tA14** and **sA14** were prepared by hydrolysis of **tE14** and **sE14**, respectively, thus eliminating the need to separate the long chain carboxylic acid derivatives from 2,3,6,7-tetrakis(tetradecyl)phenanthrene-9,10-dione **1c**.

Solution Properties. Preliminary ^{1}H NMR studies revealed large upfield shifts in the spectra of **sA6**, **sA10**, and **sA14** with increasing concentration, which is an indication that self-assembly is occurring in solution. For systems that assemble in solution, the observed peaks typically reflect the average chemical shift of the monomer and self-assembled species, and they shift with increasing concentration as the proportion of monomer decreases.[23,24] These observations prompted us to investigate the solution behavior of compounds in series **sA**, as well as that of their methyl ester analogues (series **sE**).

^{1}H NMR dilution experiments were conducted for all compounds in series **sA** and **sE** to precisely assess the changes in chemical shifts with concentration. The three ester derivatives display only minor variations in chemical shifts with changing concentration (Figure 1A), which indicates that there is no measurable self-association occurring in the concentration range studied. In contrast, acids **sA6**, **sA10**, and **sA14** exhibit large changes in chemical shift with concentration (Figure 1B). In all cases, the signal of all aromatic protons and the acid proton are shifted upfield with increasing concentration, which is consistent with the aromatic core of one molecule residing within the shielding cone of the aromatic system of another molecule, as is the case in π-stacked systems.[25,26] Increasing the concentration shifts each signal to a different extent, which results in peak crossovers and causes the appearance of the spectra to dramatically alter over the concentration range studied.

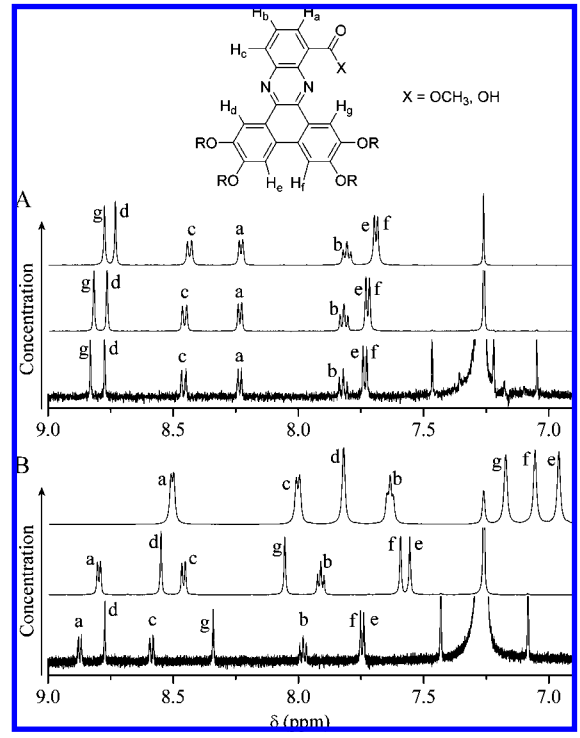

Figure 1. Aromatic region of the ^{1}H NMR spectra of molecules in series **sA** and **sE** with peak assignments. Results are shown for **sE10** and **sA10** but are representative of the entire series. Spectra were taken in $CDCl_3$ at various concentrations. (A) **sE10** at 0.1, 6.7, and 27.6 mM; (B) **sA10** at 0.1, 6.6, and 71.6 mM.

Analysis of the relative changes in chemical shifts of the aromatic protons as a function of concentration could provide insight into the geometry of the self-assembled structures. To accomplish this, it was first necessary to unambiguously assign all peaks in the aromatic region of the ^{1}H NMR spectra of molecules in series **sA** and **sE** using 2D NMR spectroscopy. ROESY showed the through-space interactions between the acid or ester protons and the two nearest aromatic protons[27] and HMBC was used to identify protons that couple to the same carbon atoms and are therefore separated by only a few chemical bonds. The combination of these two techniques allowed the reliable assignment of all aromatic peaks. These assignments are shown in Figure 1; the same proton labels are used in Figures 2 and 3.

At low concentrations, the ^{1}H NMR spectra of molecules **sA** are very similar to those of molecules **sE**, with protons *b*, *c*, *d*, *e*, and *f* having very similar chemical shifts in both series of molecules, as shown in Figure 1. The chemical shifts of protons *a* and *g* are more influenced by the change of substituent from a methyl ester to a carboxylic acid due to their proximity to the functional group. The similarity between the spectra of mol-

(21) (a) Chapman, E.; Stephen, H. *J. Chem. Soc.* **1925**, *127*, 1791–1797. (b) Haroun, M.; Helissey, P.; Giorgi-Renault, S. *Synth. Commun.* **2001**, *31*, 2329–2334. (c) Vogel, A. I. *A Textbook of Practical Organic Chemistry Including Qualitative Organic Analysis*; 3rd. ed.; Longmans Greens and Co.: London, 1956; p 966−967;(d) White, A. W.; Almassy, R.; Calvert, A. H.; Curtin, N. J.; Griffin, R. J.; Hostomsky, Z.; Maegley, K.; Newell, D. R.; Srinivasan, S.; Golding, B. T. *J. Med. Chem.* **2000**, *43*, 4084–4097.

(22) Mohr, B.; Enkelmann, V.; Wegner, G. *J. Org. Chem.* **1994**, *59*, 635–638.

(23) (a) Connors, A. C. *Binding Constants-The Measurement of Molecular Complex Stability*; John Wiley & Sons, Inc.: New York, 1987. (b) Gardner, M.; Guerin, A. J.; Hunter, C. A.; Michelsen, U.; Rotger, C. *New J. Chem.* **1999**, *23*, 309–316. (c) Zouvelekis, D.; Yannakopoulou, K.; Mavridis, I. M.; Antoniadou-Vyza, E. *Carbohydr. Res.* **2002**, *337*, 1387–1395.

(24) (a) Baxter, N. J.; Williamson, M. P.; Lilley, T. H.; Haslam, E. *J. Chem. Soc., Faraday Trans.* **1996**, *92*, 231–234. (b) Latypov, S.; Fakhfakh, M. A.; Jullian, J.-C.; Franck, X.; Hocquemiller, R.; Figadère, B. *Bull. Chem. Soc. Jpn.* **2005**, *78*, 1296–1301. (c) Mitra, A.; Seaton, P. J.; Assarpour, R. A.; Williamson, T. *Tetrahedron* **1998**, *54*, 15489–15498.

(25) Pavia, D. L.; Lampman, G. M.; Kriz, G. S. *Introduction to Spectroscopy*, 3rd ed.; Books/Cole Thompson Learning Inc.: Toronto, Canada, 2001.

(26) Silverstein, R. M.; Webster, F. X. *Spectrometric Identification of Organic Compounds*, 6th ed.; John Wiley & Sons, Inc.: New York, 1998.

(27) The ROESY spectra used for the assignments were acquired at high concentration to shorten experiment times. For **sA10**, an additional ROESY spectrum was obtained at low concentration and displayed equivalent couplings, confirming that the cross peaks seen at high concentration reflect intramolecular interactions.

(28) See Supporting Information for details.

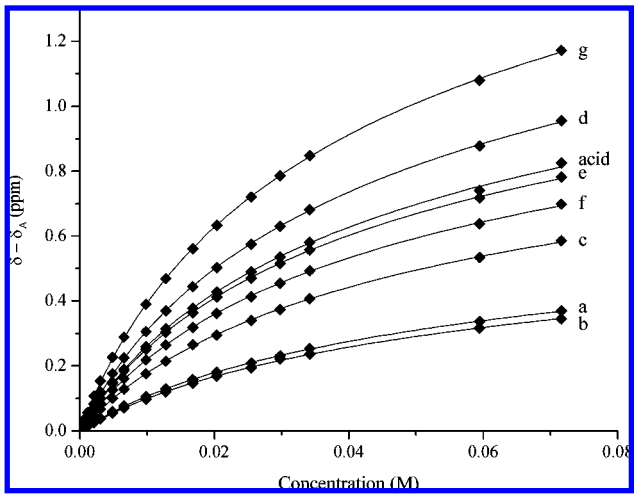

Figure 2. Changes in chemical shift versus concentration in $CDCl_3$ for **sA10**. Letters refer to proton assignments shown in Figure 1, and *acid* designates the proton on the carboxylic acid. Fitting curves were calculated with Origin 6.1 based on the dimer model.[28]

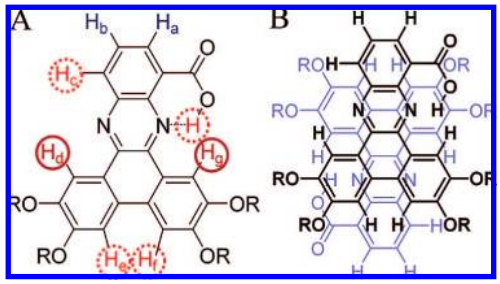

Figure 3. (A) Pattern of variation in chemical shift with concentration: H_x, protons that exhibit largest shift; H_x, protons that exhibit medium shift; H_x, protons that exhibit smallest shift. (B) Proposed structure of offset π-stacked dimers.

ecules **sE**, which exhibit no appreciable concentration dependence and therefore do not appear to self-assemble in solution, and the low concentration spectra of molecules **sA** supports the conclusion that molecules **sA** are present as monomers at low concentrations.

NMR dilution results were analyzed using the dimer model, which assumes that only monomers and dimers are present to the exclusion of higher order aggregates.[23] It is described by

$$\delta - \delta_A = \frac{1 + 4K_{dim}[A]_0 - \sqrt{1 + 8K_{dim}[A]_0}}{4K_{dim}[A]_0}(\delta_{dim} - \delta_A) \quad (1)$$

where δ is the observed chemical shift, δ_A is the chemical shift of the monomer, K_{dim} is the dimerization constant, $[A]_0$ is the total concentration of molecule in solution, and δ_{dim} is the chemical shift of the dimer.

The chemical shifts of the monomers (δ_A) were estimated by linear regression on the first five data points for each curve (between approximately 0.05 and 1 mM), and were always very close to the values obtained at the lowest measured concentration (0.007 ppm difference or less). Plots of ($\delta - \delta_A$) as a function of total concentration were fitted to eq 1, setting K_{dim} and ($\delta_{dim} - \delta_A$) as variable parameters; Figure 2 shows the fits for **sA10**, and Table 1 summarizes the calculated dimerization constants. The obtained fits were very good, with reduced chi-squared values between 6.0×10^{-5} and 1.4×10^{-6}; the system seems to be accurately described by the dimer model.

Table 1. Dimerization Constants Calculated from NMR Dilution Experiments

	K_{dim} (M^{-1})[a]	standard deviation
sA6	7	1
sA10	9	1
sA14	10	1

[a] Dimerization constants calculated by averaging results obtained from eight peaks (seven aromatic protons and acid proton) for each molecule.

For each molecule, a dimerization constant was obtained for each of the aromatic protons and the carboxylic acid proton, and the average of these eight results was calculated. Values for all eight observed protons are in mutual agreement, which is a further indication that the model accurately describes the system. The calculated dimerization constants are on the order of 1×10^1 M^{-1} and display a small increase with increasing chain length.

Figure 2 highlights the fact that some protons shift much more than others, which reflects the extent to which the environment around each proton is modified in the dimer. It was found that protons *g* and *d* shift most dramatically with increasing concentration, while protons *a* and *b* show the smallest variations (Figure 3A). This pattern does not appear to be consistent with the formation of hydrogen-bonded dimers via the carboxylic acid groups, since such complexes would be expected to lead to more substantial changes on the side of the carboxylic acid (protons *a* and *g*) and minimal perturbations on the opposite side (protons *c* and *d*), which is not what is observed. The observed changes can be explained by the formation of offset antiparallel π-stacked dimers, as illustrated in Figure 3B. This stacking would place the entire cores within each other's shielding cones, which explains why all protons are shifted upfield. The offset would cause the protons at the center of the molecule (protons *d* and *g*) to be directly above the neighboring core and those at the top (protons *a* and *b*) to be further away, which would result in the observed pattern. This model is also in agreement with general models concerning π-stacking, which predict that offset or slipped geometries are favored because they maximize attractive $\sigma-\pi$ interactions while minimizing $\pi-\pi$ repulsions.[29]

The NMR data therefore suggest that the carboxylic acids do not form hydrogen-bonded dimers, which could be explained by the formation of a competing intramolecular hydrogen bond between the OH group on the carboxylic acid and the suitably positioned pyrazinyl nitrogen atom (Figure 3A). The acid proton was therefore positioned near the pyrazinyl nitrogen atom in Figure 3, despite the fact that this corresponds to a typically unfavorable conformation of the carboxylic acid substituent.

Dynamic light scattering was also employed to study the solution behavior of compounds in series **sE** and **sA**. Hydrodynamic diameters were measured for each compound at various concentrations, as summarized in Figure 4. The sizes measured for the three acid derivatives increase with concentration, but separate peaks corresponding to the monomer and dimer are not observed. Because these molecules are disc-shaped rather than spherical, the measured sizes correspond to the diameter of a sphere having the same translational diffusion speed.[30] The

(29) Hunter, C. A.; Sanders, J. K. M. *J. Am. Chem. Soc.* **1990**, *112*, 5525–5534.
(30) (a) Pecora, R. *J. Nanopart. Res* **2000**, *2*, 123–131. (b) Schmitz, K. S. *An Introduction to Dynamic Light Scattering by Macromolecules*; Academic Press, Inc.: Boston, MA, 1990.

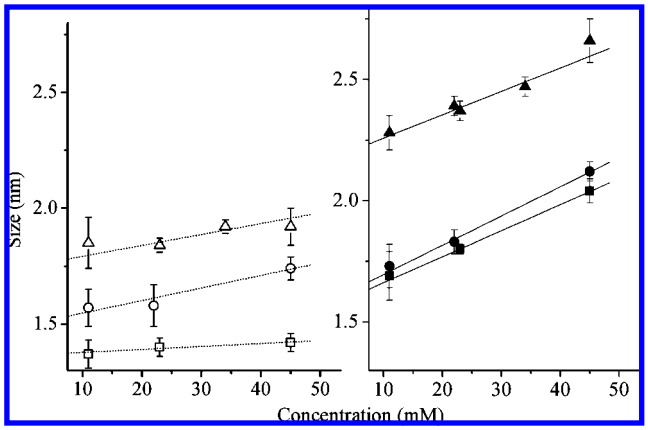

Figure 4. Hydrodynamic diameters of molecules in series **sE** and **sA** (□, **sE6**; ○, **sE10**; △, **sE14**; ■, **sA6**; ●, **sA10**; ▲, **sA14**) measured by DLS in $CHCl_3$. Error bars show the 95% confidence level after 24 measurements.

proposed π-stacked dimer is expected to have only a slightly higher hydrodynamic diameter than a monomer, hence it is not surprising that the two populations are not resolved. The sizes measured for such samples therefore reflect the presence of both species, and increase with an increasing dimer to monomer ratio. The observed increases in size with concentration are consistent with a rise in the proportion of dimers at higher concentrations.

The absence of a significant concentration effect in the case of the three ester derivatives indicates that there is no self-assembly occurring in these cases. Furthermore, the diameters of the acid derivatives are consistently larger than those of their ester counterparts having the same alkoxy chain length, which again points to the presence of dimers in the samples of **sA6**, **sA10**, and **sA14** even at the lowest concentrations probed by DLS, which are approximately two orders of magnitude higher than the lowest concentrations investigated by NMR.

Self-assembly in solution was not observed for any of the other discotic molecules having the same aromatic core,[31] suggesting that the carboxylic acid group plays an important role in the formation of the π-stacked dimers. Figure 3B shows the carboxylic acid positioned for intramolecular hydrogen bonding with the pyrazine nitrogen atom, but it could also easily form an intermolecular hydrogen bond with the oxygen atoms of an ether linkage or the π-system of an aromatic ring[32] from the neighboring molecule without greatly changing its geometry, perhaps as part of a three-centered hydrogen bond also involving the pyrazine nitrogen atom. It is therefore possible that the π-stacked dimers are further stabilized by hydrogen bonding.

Liquid Crystalline Behavior. All new compounds were studied by differential scanning calorimetry (DSC) and polarized optical microscopy (POM). Typical liquid crystalline textures are shown in Figure 5. Liquid crystalline compounds were also examined by variable temperature X-ray diffraction (XRD).[33] Phase transition temperatures, XRD data, and lattice parameters of all new compounds are summarized in Tables 2−7 along with those of previously reported compounds **tN6**, **tE6**, **tE10**, **tA6**, and **tA10**.

(31) Compounds **tA6**, **tA10**, and **tA14** have severely limited solubility and could therefore only be observed at very low concentrations.
(32) Jeffrey, G. A. *An Introduction to Hydrogen Bonding*, 1st ed.; Oxford University Press: Oxford, U.K., 1997.
(33) Using a Rigaku RAXIS rapid diffractometer and a furnace that was manufactured in house, see: (a) Lavigueur, C.; Foster, E. J.; Williams, V. E. *J. Appl. Crystallogr.* **2008**, *41*, 214–216.

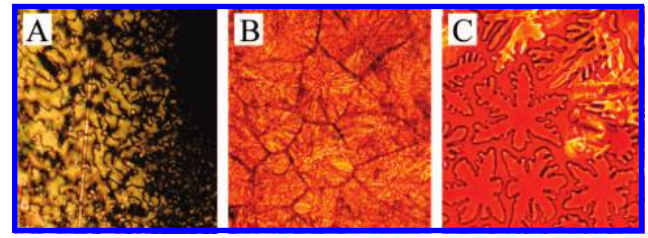

Figure 5. Representative textures observed by POM for new liquid crystalline compounds. (A) **tA14**, 180 °C, N, 100× magnification; (B) **tA14**, 153 °C, Col_r, 100× magnification; (C) **sA6**, 256 °C, Col_h, 400× magnification.

Table 2. Phase Behavior of Carboxylic Acid-Substituted Compounds

Cmpd	Phase[b]	T_t/°C (ΔH/J g^{-1})[a]	Phase[b]
tA6[c]	Cr	173 (66) → Col_h ⇌ 263 (19) / 257 (-17)	I
tA10[c]	Cr	122 (33) → Col_r ⇌ 196 (10) / 191 (-10)	N ⇌ 209 (1) / 207 (-1) I
tA14[d]	Cr	47 (39) / 41 (-37) ⇌ Col_r ⇌ 154 (3) / 150 (-3)	N ⇌ 193 (1) / 191 (-1) I
sA6	Cr	88 (13) → Col_h ⇌ 260 (9) / 256 (-9)	I
sA10	Cr	107 (26) → Col_h ⇌ 242 (6) / 239 (-5)	I
sA14	Cr	85 (40) / 41 (-51) ⇌ Col_h ⇌ 210 (5) / 207 (-5)	I

[a] Transition temperatures and enthalpies determined by DSC on first heating (scan rate = 5 °C/min). [b] Cr = crystal, Col_h = hexagonal columnar, Col_r = rectangular columnar, N = nematic, I = isotropic liquid. [c] Previously reported in ref 11. [d] Values reported are from second heating, Cr-to-Col_r transition not seen on first heating.

The DSC traces of **sE6**, **sE10**, and **sE14** each exhibited a single peak both on heating and cooling, indicating that they melt directly from crystalline solids to isotropic liquids without the formation of liquid crystalline phases. DSC investigation of **tA14** revealed three phase transitions both on heating and cooling. Upon cooling from the isotropic liquid, **tA14** displayed by POM a texture characteristic of a nematic phase (N) followed by a columnar phase at lower temperatures (Figure 5A,B), which was identified as a rectangular columnar phase by XRD. The X-ray diffractogram displayed two intense and two weaker low-angle peaks that indexed to the (200), (110), (400), and (020) reflections of a rectangular lattice. Broad peaks were also observed corresponding to distances of approximately 4.5 and 3.5 Å, which were attributed to the alkyl chain halo and to the π-stacking distance, respectively.

Examination of **sN14** by DSC revealed the presence of a single peak upon heating and two distinct peaks on cooling, indicative of the formation of a monotropic liquid crystalline phase. All remaining compounds (**tN14**, **sN6**, **tE14**, **sA6**, **sA10**, and **sA14**) displayed two peaks both on heating and on cooling. POM revealed that upon cooling from the isotropic liquid, all seven compounds displayed dendritic textures with approxi-

Table 3. X-Ray Diffraction Data of Carboxylic Acid-Substituted Compounds

	temp (°C)	*d*-spacing (Å)	Miller index (*hkl*)	phase (lattice constants)
tA6[a]	175	16.6	(100)	Col_h
		4.2	*alkyl halo*	(a = 19.1 Å)
		3.6	$\pi-\pi$	
tA10[a]	140	22.7	(200)	Col_r
		17.7	(110)	(a = 45.4 Å)
		11.6	(400)	(b = 19.5 Å)
		4.4	*alkyl halo*	
		3.6	$\pi-\pi$	
tA14	100	27.0	(200)	Col_r
		19.7	(110)	(a = 54.0 Å)
		13.7	(400)	(b = 21.1 Å)
		10.6	(020)	
		4.2	*alkyl halo*	
		3.8	$\pi-\pi$	
sA6	100	17.0	(100)	Col_h
		9.9	(110)	(a = 19.7 Å)
		4.3	*alkyl halo*	
		3.5	$\pi-\pi$	
sA10	165	20.6	(100)	Col_h
		11.8	(110)	(a = 23.8 Å)
		10.2	(200)	
		4.2	*alkyl halo*	
		3.5	$\pi-\pi$	
sA14	150	23.1	(100)	Col_h
		13.4	(110)	(a = 26.7 Å)
		11.6	(200)	
		4.6	*alkyl halo*	
		3.5	$\pi-\pi$	

[a] Previously reported in ref 11.

mately 6-fold symmetric domains characteristic of hexagonal columnar phases (Figure 5C). The X-ray diffractogram of each of these compounds showed broad peaks corresponding to the alkyl chain halo and to the π-stacking distance (~3.5 Å) as well as an intense low-angle peak which was assigned as the (100) reflection of a hexagonal lattice. For all compounds except **sN6**, a second peak indexing to the (110) reflection was also observed, which confirmed the assignment of a hexagonal columnar phase. For **tN14**, **tE14**, **sA10**, and **sA14**, further peaks indexing to the (200) reflection were also observed.

For each series examined in the present study, both the melting and clearing temperatures decrease with increasing chain length, which is consistent with the general trends observed for other series of discotic mesogens.[11,13,14] Within series **tN**, **tE**, and **sA**, the clearing temperatures are typically lowered to a greater extent than the melting temperatures, which results in a narrowing of the liquid crystalline phase range. In series **sN**, increasing the alkoxy chain length from **sN6** to **sN14** causes the complete disappearance of the liquid crystalline phase on heating, leaving only a narrow monotropic phase observed on cooling.

We have previously reported that changing the chain length has dramatic effects on the phase behavior of the elliptical dimers formed by compounds in series **tA**, with the type of mesophases observed changing with alkoxy chain length.[11] It was also noted that increasing the chain length broadened the nematic phase range within this series. This trend continues for the longer chain derivative **tA14** prepared for the present study, which has a nematic phase that persists over a 39 °C range as compared to a range of only 13 °C for the nematic phase of **tA10**. The lowering of the melting temperatures was also very pronounced in the case of **sA14** and **tA14**, where the liquid crystalline phases are observed close to room temperature. **sA14** is liquid crystalline down to 41 °C on cooling although its melting temperature is considerably higher at 85 °C, while **tA14** has a melting point of only 47 °C, and also maintains its columnar phase down to 41 °C on cooling.

Before addressing the effects of functional group position on the phase behavior of carboxylic acid derivatives, it is useful to examine the perturbations induced by relocating non-hydrogen bonding substituents. Moving a nitro group from the top of the molecule in **tN6** to the side in **sN6** leads to a dramatic lowering of the clearing temperature from 229 to 175 °C, whereas the melting temperature remains essentially unchanged. As a result, the hexagonal columnar phase of **sN6** has a much narrower temperature range (42 °C) than that of **tN6** (98 °C). A destabilization of the columnar phase is also observed in the case of the longer chain derivatives, **tN14** and **sN14**; the former has an enantiotropic hexagonal columnar phase from 107 to 136 °C, while the latter melts directly from a crystalline solid to an isotropic liquid at 115 °C, and forms only a narrow monotropic phase on cooling. The same trend was found for the ester derivatives in series **tE** and **sE**. Whereas **tE6**, **tE10**, and **tE14** form hexagonal columnar phases, **sE6**, **sE10**, and **sE14** are nonmesogenic. This effect was also noted in a previous study of the disc-shaped pyridyl derivatives **tP** and **sP**.[13] Although **tP6** and **tP10** exhibit stable hexagonal columnar phases, their isomers **sP6** and **sP10** are not liquid crystalline.

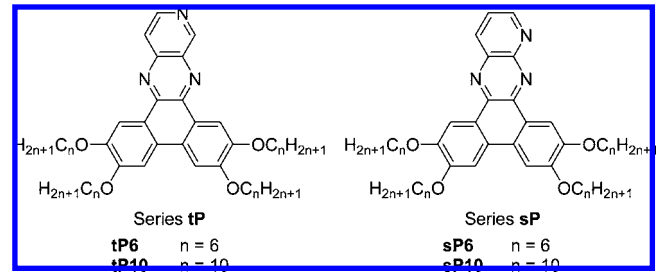

As a general rule, it appears that moving an electron-withdrawing substituent from the top of the molecule to the side destabilizes the liquid crystalline phases, which may provide key insight into the role of functional groups in the formation of these phases. We have previously suggested that electron-withdrawing groups stabilize columnar phases by minimizing $\pi-\pi$ repulsions between aromatic cores and/or by maximizing favorable dipole−dipole interactions.[16,34] To assemble into hexagonally ordered nanostructures, it is anticipated that these low symmetry molecules order antiferroelectrically, meaning that neighboring molecules within a column align antiparallel to one another (Figure 6A). This arrangement, which is consistent with the intercolumnar distances measured by XRD, would be favored by a large dipole along the long axis of the core (μ_y). Molecules with an electron-withdrawing group on the top of the core (e.g., **tN** and **tE**) will have larger components of their dipole in the *y*-direction, as schematically illustrated in Figure 6B. These molecules will thus be more stabilized in an antiparallel orientation than isomers with substituents on the

(34) Several other groups have also rationalized the effects of substituents on the stability of columnar phases in terms of dipole-dipole interaction: (a) Bushby, R. J.; Lozman, O. R. *Curr. Opin. Colloid Interface Sci.* **2002**, *7*, 343–354. (b) Laschat, S.; Baro, A.; Steinke, N.; Giesselmann, F.; Hägele, C.; Scalia, G.; Judele, R.; Kapatsina, E.; Sauer, S.; Schreivogel, A.; Tosoni, M. *Angew. Chem., Int. Ed. Engl.* **2007**, *46*, 4832–4887. (c) Kishikawa, K.; Furusawa, S.; Yamaki, T.; Kohmoto, S.; Yamamoto, M.; Yamaguchi, K. *J. Am. Chem. Soc.* **2002**, *124*, 1597–1605. (d) Trzaska, S. T.; Swager, T. M. *Chem. Mater.* **1998**, *10*, 438–443.

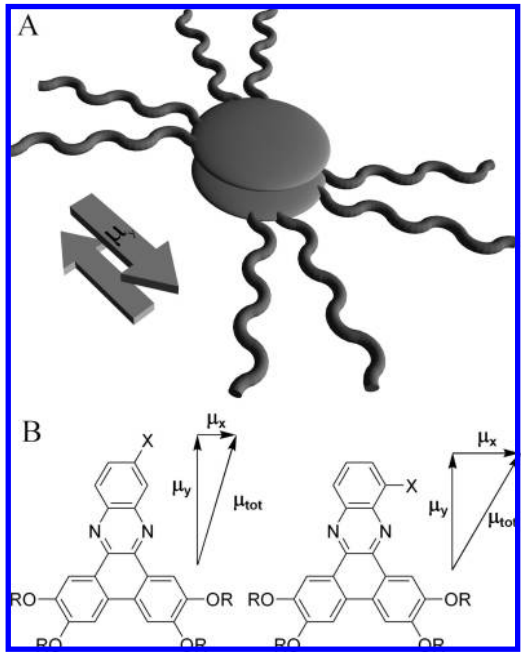

Figure 6. Schematic representation of (A) the antiparallel alignment of adjacent molecules favored by a large dipole moment along the long axis of the molecule (μ_y), (B) the effect of substituent position on molecular dipole.

side of the core (e.g., **sN** and **sE**). This hypothesis is borne out by dipole moment calculations at the AM1 level for dibenzophenazines with nitro substituents on the top or side of the core, which afforded μ_y values of 6.4 and 2.1 D, respectively.[28] Our present observations therefore provide support for earlier suggestions that dipole−dipole interactions play a critical role in stabilizing columnar phases.

The same dipole effect can explain why liquid crystalline phases are observed for disc-shaped molecules having a nitro substituent on the side of the core, but not for those having a methyl ester or the nitrogen atom of a pyridine ring at the same position, since the more electron-withdrawing nitro group will lead to a larger dipole moment and will thus further stabilize columnar phases. This is in accordance with previously observed trends concerning the nature of functional groups which had revealed that clearing temperatures increase with increasing electron-withdrawing ability of substituents.[16]

Functional group conformation may also contribute to the observed differences caused by substituent position. AM1 models of the nitro and ester derivatives indicate that these groups are approximately coplanar with the aromatic core in **tN** and **tE**, but are twisted relative to the core in **sN** and **sE**, with dihedral angles of 49° and 48°, respectively. This loss of coplanarity will diminish the electron-withdrawing abilities of the substituents and increase the steric repulsion between neighboring molecules within a column; both effects would be expected to destabilize the columnar mesophase. However, this effect would not account for the diminished propensity of **sP** to form a columnar mesophase. Moreover, because the energetic cost of these groups adopting a coplanar conformation is rather modest (0.8−1.3 kcal/mol), it seems likely that this effect is relatively small compared to that of changes in μ_y.

The carboxylic acid derivatives in series **tA** and **sA** fail to follow the trends described above. Indeed, in some cases, mesogens with a carboxylic acid group on the side of the core (**sA10** and **sA14**) actually have higher clearing temperatures than their isomers with the acid group in the top position, and in the remaining case (**sA6** versus **tA6**), there is no significant difference between the clearing temperatures. In contrast to mesogens with non-hydrogen bonding substituents, molecules **sA** also do not exhibit a narrowing of their mesophases relative to their isomers **tA**; **sA6** and **sA10** have broader liquid crystalline phase ranges than **tA6** and **tA10**, respectively. These differences suggest that factors in addition to the dipole−dipole effects described above are contributing to the mesophase stabilities of molecules in series **sA**. This hypothesis is supported by the observation that members of series **sA** have considerably higher clearing temperatures than the corresponding **sN** compounds, even though nitro substituents are far more electron-withdrawing than carboxylic acid groups, and would therefore be expected to give rise to higher dipole moments. The most likely cause of the increased stability of the mesophases of compounds **sA** is the ability of a carboxylic acid group to act as a hydrogen bond donor and/or acceptor.

A comparison of the acid-substituted compounds **tA** and **sA** also reveals differences in the types of phases formed. The acid derivatives in series **tA** having sufficiently long chains (**tA10** and **tA14**) form both nematic and rectangular columnar mesophases. As already noted, we have proposed that this behavior results from the formation of elliptical hydrogen-bonded dimers.[11] In contrast, the molecules in series **sA** exclusively form hexagonal columnar mesophases, regardless of chain length. The observed intercolumnar distances are consistent with columns formed by stacks of single molecules and closely agree with those measured for molecules in series **tN**, **sN**, and **tE**, none of which can hydrogen bond. The lattice parameters measured for molecules in series **sA** are therefore not consistent with columns formed by stacked hydrogen-bonded dimers.

FTIR spectroscopy was used to further probe hydrogen bonding within the liquid crystalline phases of carboxylic acid and methyl ester-substituted compounds.[35] Almost no variation in peak positions was observed with changing alkoxy chain length. Variable temperature FTIR spectroscopy was used to further characterize **sA6**, **sA10**, **sA14**, **sE10** and **tA10** up to 250 °C, which spanned the Cr-LC-I transitions for **sA10**, **sA14**, **sE10** and **tA10**. No major changes in the spectra and no discontinuities were observed with increasing temperatures for any of these molecules, hence comparisons were made with the room temperature spectra.

The bands that best reflect the presence or absence of hydrogen bonding in carboxylic acid derivatives are the hydroxyl and carbonyl stretches.[26] No O−H stretch was clearly observed for any acid derivative. It is possible that the C−H stretching vibrations bury the O−H stretches since these molecules have four long alkoxy chains corresponding to between 52 and 113 C−H bonds involving sp^3-hybridized carbon atoms compared to a single carboxylic acid group. If this is the case, then the O−H stretches would be located around 2900 cm^{-1}, in the region corresponding to hydrogen-bonded OH groups. In comparison, free hydroxyl groups have a stretching band near 3500 cm^{-1}, a region in which no absorption is observed for any of the carboxylic acid-substituted molecules.

The position of the carbonyl stretch also gives valuable information about hydrogen bonding; C═O stretching frequen-

(35) We attempted probe the changes in the FTIR spectra of these compounds in solution with varying concentration; unfortunately, useful spectra could only be obtained at higher concentrations, where a significant fraction of molecules are expected to exist as dimers for compounds in series **sA**.

Table 4. Phase Behavior of Methyl Ester-Substituted Compounds

Cmpd	Phase[b]	T_t/°C (ΔH/J g^{-1})[a]		Phase[b]
tE6[c]	Cr	111 (39) →	Col_h	200 (5) → / ← 197 (-5)	I
tE10[c]	Cr	98 (61) →	Col_h	137 (3) → / ← 132 (-3)	I
tE14	Cr	77 (46) → / ← 52 (-62)	Col_h	98 (2) → / ← 94 (-2)	I
sE6	Cr	158 (70) → / ← 129 (-79)	I		
sE10	Cr	127 (78) → / ← 99 (-69)	I		
sE14	Cr	110 (42) → / ← 87 (-53)	I		

[a] Transition temperatures and enthalpies determined by DSC on first heating (scan rate = 5 °C/min). [b] Cr = crystal, Col_h = hexagonal columnar, I = isotropic liquid. [c] Previously reported in ref 11.

Table 5. X-Ray Diffraction Data of Liquid Crystalline Methyl-Ester-Substituted Compounds

	temp (°C)	*d*-spacing (Å)	Miller index (*hkl*)	phase (lattice constants)
tE6[a]	150	17.3	(100)	Col_h
		4.3	*alkyl halo*	(a = 20.0 Å)
		3.5	$\pi-\pi$	
tE10[a]	140	18.9	(100)	Col_h
		4.4	*alkyl halo*	(a = 22.4 Å)
		3.5	$\pi-\pi$	
tE14	75	23.0	(100)	Col_h
		13.3	(110)	(a = 26.6 Å)
		11.5	(200)	
		4.5	*alkyl halo*	
		3.5	$\pi-\pi$	

[a] Previously reported in ref 11.

cies for compounds in series **tE**, **sE**, **tA**, and **sA** are summarized in Table 8. It is however important to remember that the position of carbonyl stretches is influenced not only by hydrogen bonding but also by conjugation to an aromatic system, and that moving the substituent to a different position on the core will cause a shift in the vibration frequency that may not be attributable to a change in hydrogen bonding. This effect can be more readily observed in the ester-substituted molecules where hydrogen bonding is not involved. In this case, the C=O stretch shifts to lower frequency when the functional group is moved to the side of the core, indicating that conjugation with the aromatic core is increased.[26]

An analogous shift would be expected in the acid-substituted molecules if variation in the extent of conjugation with the aromatic core was also the main factor in determining the position of the carbonyl stretch. The opposite occurs, the C=O stretch being shifted to higher frequency when the acid group is on the side of the core (see Table 8). This can be explained by the carbonyl groups in series **tA** serving as hydrogen bond acceptors, and those in series **sA** not being involved in hydrogen bonding, or at least to a much lesser extent.[26]

Two different models are consistent with the conclusion that the hydroxyl groups in **sA6**, **sA10**, and **sA14** are involved in hydrogen bonding, but that the carbonyls are not. It is possible that the carboxylic acid groups form intramolecular hydrogen bonds with the pyrazinyl nitrogen atoms that are ideally positioned to serve as hydrogen-bond acceptors. Alternatively, intermolecular hydrogen bonds may be formed in which the hydroxyl groups act as hydrogen-bond donors, and the π-system of aromatic rings or the oxygen atoms of the ether linkages of neighboring molecules within the columns act as hydrogen-bond acceptors. We have no clear evidence that would distinguish between these two potential intermolecular hydrogen-bond acceptors; either case would result in hydrogen bonding up and down the columns without involvement of the carbonyl group, which would explain the high stability of the columnar phases, the position of the C=O stretch, and the measured intercolumnar distances.

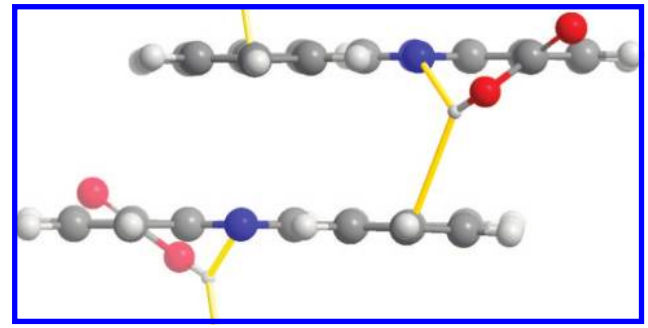

Figure 7. Schematic representation of the proposed three-centered hydrogen bonding (highlighted in gold) between antiparallel π-stacked molecules within a column with hydroxyl groups as hydrogen-bond donors, and both pyrazine nitrogen atoms (intramolecular bond) and π-systems of aromatic rings (intermolecular bond) as hydrogen-bond acceptors. The alkoxy chains have been omitted for clarity. Oxygen is shown in red, nitrogen in blue, carbon in dark gray, and hydrogen in pale gray.

It is of course possible that both models, intramolecular and intermolecular hydrogen bonding, are occurring concurrently with the formation of three-centered hydrogen bonds between hydroxyl donors, pyrazinyl nitrogen atoms on the same molecule, and oxygen atoms or the π-system of the aromatic rings on a neighboring molecule. Figure 7 shows the proposed structure of a 3-centered hydrogen bond involving the π-system; for simplicity, the alternative possibility in which an oxygen atom acts as the acceptor has not been represented, since this structure would be geometrically similar to the one shown.

The proposed network of hydrogen bonds in the liquid crystalline phase does not involve the formation of a cyclic carboxylic acid dimer, which is a commonly observed motif in the solid state.[36,37] However, other binding modes are known, especially in the presence of competing hydrogen bond acceptors.[36] Formation of catemer structures, in which carboxylic acids hydrogen bond into infinite chains rather than dimers, have also been observed in a number of cases.[38] The proposed structure involves intracolumnar hydrogen bonding, which has been observed in other systems and has been found to enhance the attractive interactions that promote columnar ordering.[39,40] In a system studied by Ivanov and co-workers, hydrogen bonding between neighboring molecules within a column led

(36) Steiner, T. *Acta Crystallogr., Sect. B* **2001**, *57*, 103–106.
(37) Steiner, T. *Angew. Chem., Int. Ed.* **2002**, *41*, 48–76.
(38) (a) Beyer, T.; Price, S. L. *J. Phys. Chem. B* **2000**, *104*, 2647–2655. (b) Davis, J. L.; Barteau, M. A. *Langmuir* **1989**, *5*, 1299–1309. (c) Sørensen, H. O.; Larsen, S. *Acta Crystallogr., Sect. B* **2003**, *59*, 132–140.

Table 6. Phase Behavior of Nitro-Substituted Compounds

Cmpd	Phase[b]	T_t/°C (ΔH/J g^{-1})[a]	Phase[b]
tN6[c]	Cr	131 (67) / 102 (-53)	Col_h	229 (8) / 226 (-7)	I
tN14	Cr	107 (66) / 80 (-71)	Col_h	136 (1) / 131 (-1)	I
sN6	Cr	132 (37) / 78 (-40)	Col_h	175 (7) / 172 (-7)	I
sN14	Cr	115 (41) / 98 (-40)	Col_h	109 (-2)	I

[a] Transition temperatures and enthalpies determined by DSC on first heating (scan rate = 5 °C/min); [b]Cr = crystal, Col_h = hexagonal columnar, I = isotropic liquid; [c]previously reported in ref 16.

Table 7. X-Ray Diffraction Data of Nitro-Substituted Compounds

	temp (°C)	*d*-spacing (Å)	Miller index (*hkl*)	phase (lattice constants)
tN6[a]	150	16.7	(100)	Col_h
		9.3	(110)	(a = 19.2 Å)
		4.7	*alkyl halo*	
		3.5	$\pi-\pi$	
tN14	100	23.1	(100)	Col_h
		13.4	(110)	(a = 26.7 Å)
		11.6	(200)	
		4.4	*alkyl halo*	
		3.5	$\pi-\pi$	
sN6	150	17.0	(100)	Col_h
		4.4	*alkyl halo*	(a = 19.6 Å)
		3.6	$\pi-\pi$	
sN14	108	23.1	(100)	Col_h
		13.3	(110)	(a = 26.7 Å)
		4.3	*alkyl halo*	
		3.5	$\pi-\pi$	

[a] Previously reported in ref 16.

Table 8. Position of C=O Stretches for Series **tE**, **sE**, **tA**, and **sA**

	C=O stretch (cm^{-1})[a]
tE10	1727
sE10	1709
tA10	1693
sA10	1742

[a] Observed at room temperature. Alkoxy chain length does not impact this stretching frequency, hence results are representative of the entire series.

to π-stacking distances as small as 3.2 Å, an attractive feature since short $\pi-\pi$ contacts lead to high charge carrier mobilities.[40] The π-stacking distances measured in the present system are larger, but it is interesting to note that the distances are slightly shorter for **sA6**, **sA10**, and **sA14** (3.5 Å in all cases) than for **tA6**, **tA10**, and **tA14** (3.6, 3.6, and 3.8 Å, respectively). This small reduction in π-stacking distances may be an additional indication that there are weak intermolecular hydrogen bonds within the columns.

The models developed to explain the self-assembly of molecules in series **sA** in the liquid crystalline state and in solution are remarkably similar. Both studies led to the conclusion that molecules self-assemble through antiparallel offset π-stacking, as shown in Figures 4 and 7. In both cases, the formation of three-centered hydrogen bonds between the hydroxyl groups and both a pyrazinyl nitrogen atom on the same molecule and an aromatic ring or an oxygen atom on a neighboring molecule is proposed to be an important factor in increasing the stability of the self-assembled structures. These interactions lead to high clearing temperatures in the liquid crystalline state and to self-assembly in solution. In the columnar phases, it is expected that each molecule will form a single hydrogen bond with each of its neighbors, as illustrated in Figure 7, thus allowing hydrogen bonding to extend along the columns. On the other hand, it appears that only dimers are formed in solution, which is perhaps not surprising given the greater entropic cost of assembling more extended structures under these conditions.

Conclusion

The molecules studied herein provide insight into the effects of the position of functional groups on mesogenic properties, which may prove useful to the rational design of liquid crystalline materials. We have demonstrated that moving a substituent to the side of the core generally reduces the stability of columnar liquid crystalline phases, most likely due to a reduction of dipole−dipole interactions that favor antiferroelectric alignment within the columns. This effect was not observed, however, in the case of carboxylic acid groups. When a carboxylic acid group was placed near the top of the core of a disc-shaped molecule, elliptical dimers were formed giving rise to nematic and columnar rectangular liquid crystalline phases. Moving this group to the side of the core eliminates hydrogen-bonded dimers in favor of hydrogen bonding along the (001) direction, that is, within the columns, leading to hexagonal columnar liquid crystalline phases having broad phase ranges and high clearing temperatures. These carboxylic acid derivatives are also observed to self-assemble in solution in a geometry very similar to that of the columnar phases, forming antiparallel offset π-stacked dimers.

The presence of hydrogen bonding within the columns of the mesophases of molecules in series **sA** leads to liquid crystalline phases that are stable over remarkably broad temperature ranges. The use of long alkoxy chains (n = 14) also gave rise to potentially useful characteristics, such as a dramatic broadening of the nematic phase range for **tA14** and a lowering of the liquid crystalline phase range close to room temperature for **tA14** and **sA14**. Increasing the length of the alkyl chains on a discotic mesogen typically depresses the transition temperatures and leads to narrower liquid crystalline phase ranges.[14] Although lowering the melting point may be an attractive design strategy for room temperature columnar phases, progressive narrowing of the phase ranges is clearly not desirable. In contrast, while the acids in series **tA** exhibit a trend toward lower melting points with increasing chain length, the columnar phase range of **tA14** is actually broader than that of either **tA6** or **tA10**. Likewise, whereas the mesophase ranges in series **sA** do become narrower with increasing chain length, this effect is far less pronounced than for other series (e.g., **tE**, **tN** or **sN**), and

(39) (a) Palma, M.; Levin, J.; Debever, O.; Geerts, Y.; Lehmann, M.; Samori, P. *Soft Matter* **2008**, *4*, 303–310. (b) Nguyen, T. Q.; Bushey, M. L.; Brus, L. E.; Nuckolls, C. *J. Am. Chem. Soc.* **2002**, *124*, 15051–15054. (c) Albouy, P. A.; Guillon, D.; Heinrich, B.; Levelut, A. M.; Malthête, J. *J. Phys. II* **1995**, *5*, 1617–1634.

(40) Gearba, R. I.; Lehmann, M.; Levin, J.; Ivanov, D. A.; Koch, M. H. J.; Barberá, J.; Debije, M. G.; Piris, J.; Geerts, Y. H. *Adv. Mater.* **2003**, *15*, 1614–1618.

sA14 has a columnar phase over a 125 °C temperature range. Thus, both series of acid derivatives (**tA** and **sA**) appear to be promising candidates for future investigation into even longer chain derivatives.

Acknowledgment. We gratefully acknowledge the Natural Sciences and Engineering Research Council of Canada (NSERC), le Fonds québécois de la recherche sur la nature et les technologies (FQRNT), and Simon Fraser University for funding; Dr. Andrew Lewis and Mr. Yilin Zhang for assistance with the NMR experiments; and Mr. Mei-Keng Yang and Mr. Frank Haftbaradaran for carrying out microanalysis.

Supporting Information Available: Experimental details including synthesis and characterization of all new compounds; peak assignments using 2D NMR experiments; ^{1}H NMR dilution experiments results along with derivation of the dimer model, fitting technique, and detailed dimerization constants; dynamic light scattering experiments and interpretation of results; variable temperature FTIR spectra; calculations of dipole moments and molecular conformations. This material is available free of charge via the Internet at http://pubs.acs.org.

JA803406K